Supplementary Materials

Probabilistic risk assessment of gold nanoparticles after intravenous administration by integrating *in vitro* and *in vivo* toxicity with physiologically based pharmacokinetic modeling

Yi-Hsien Cheng[1], Jim E Riviere[1], Nancy A Monteiro-Riviere[2], Zhoumeng Lin[1,*]

[1] Institute of Computational Comparative Medicine (ICCM), Department of Anatomy and Physiology, College of Veterinary Medicine, Kansas State University, Manhattan, KS 66506, USA; [2] Nanotechnology Innovation Center of Kansas State (NICKS), Department of Anatomy and Physiology, College of Veterinary Medicine, Kansas State University, Manhattan, KS 66506, USA

Yi-Hsien Cheng: yhcheng1987@ksu.edu; Jim E. Riviere: jriviere@ksu.edu

Nancy A. Monteiro-Riviere: nmonteiro@ksu.edu; Zhoumeng Lin: zhoumeng@ksu.edu

* Corresponding author: Institute of Computational Comparative Medicine (ICCM), Department of Anatomy and Physiology, College of Veterinary Medicine, Kansas State University, 1800 Denison Avenue, P200 Mosier Hall, Manhattan, KS 66506, USA. Email: zhoumeng@ksu.edu. Phone: +1-785-532-4087. Fax: +1-785-532-4953.

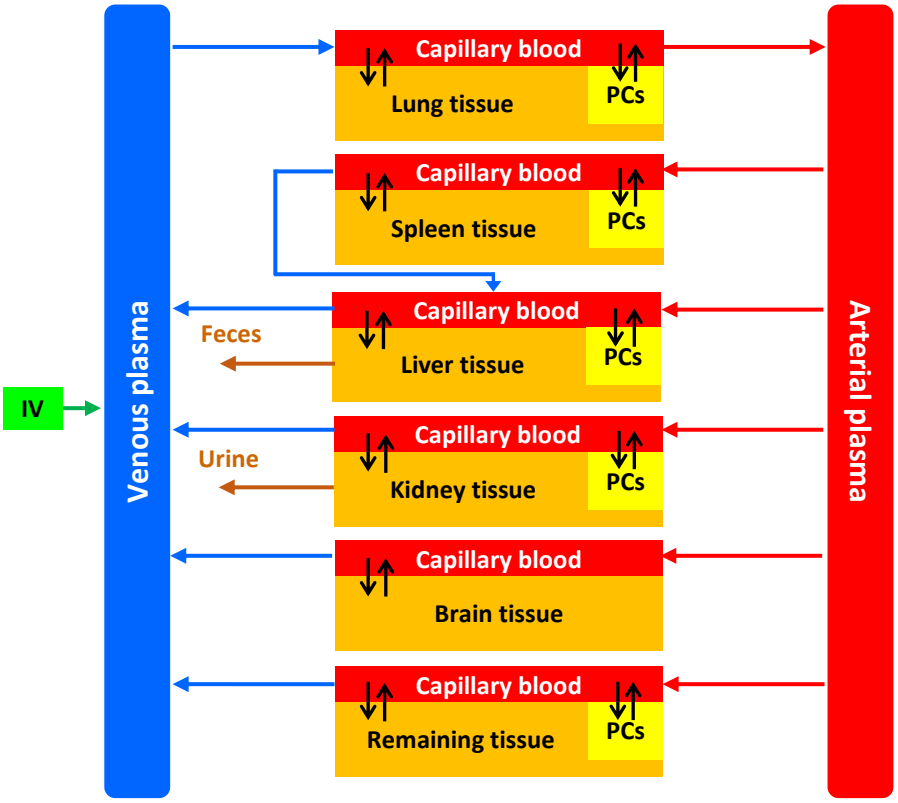

Figure S1. Schematic showing human AuNP-PBPK model following IV administration. This model structure was adapted from our earlier PBPK model for AuNPs in mice, rats, pigs, and humans (Lin et al., 2016a).

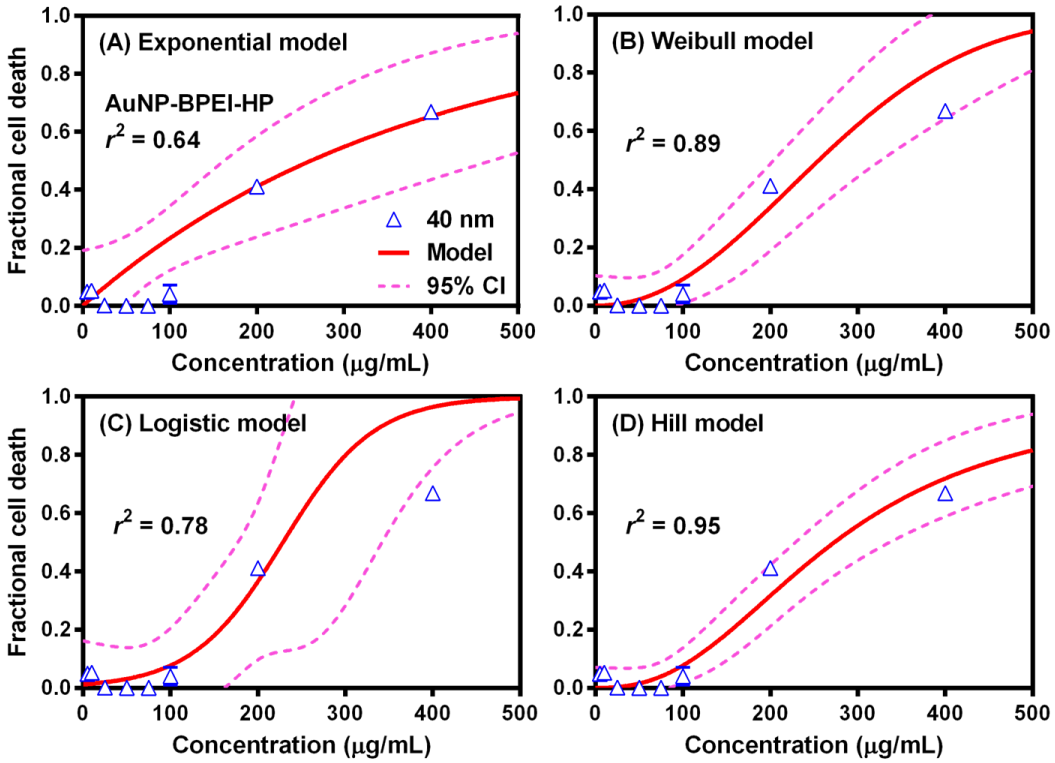

Figure S2. Comparison among fitted dose-response relationships describing concentration-dependent cell death fraction in hepatocytes exposed to 40 nm AuNP-BPEI-HP using (A) exponential, (B) Weibull, (C) Logistic, and (D) Hill model, respectively. AuNP, gold nanoparticle; BPEI, branched polyethylenimine; HP, human plasma proteins.

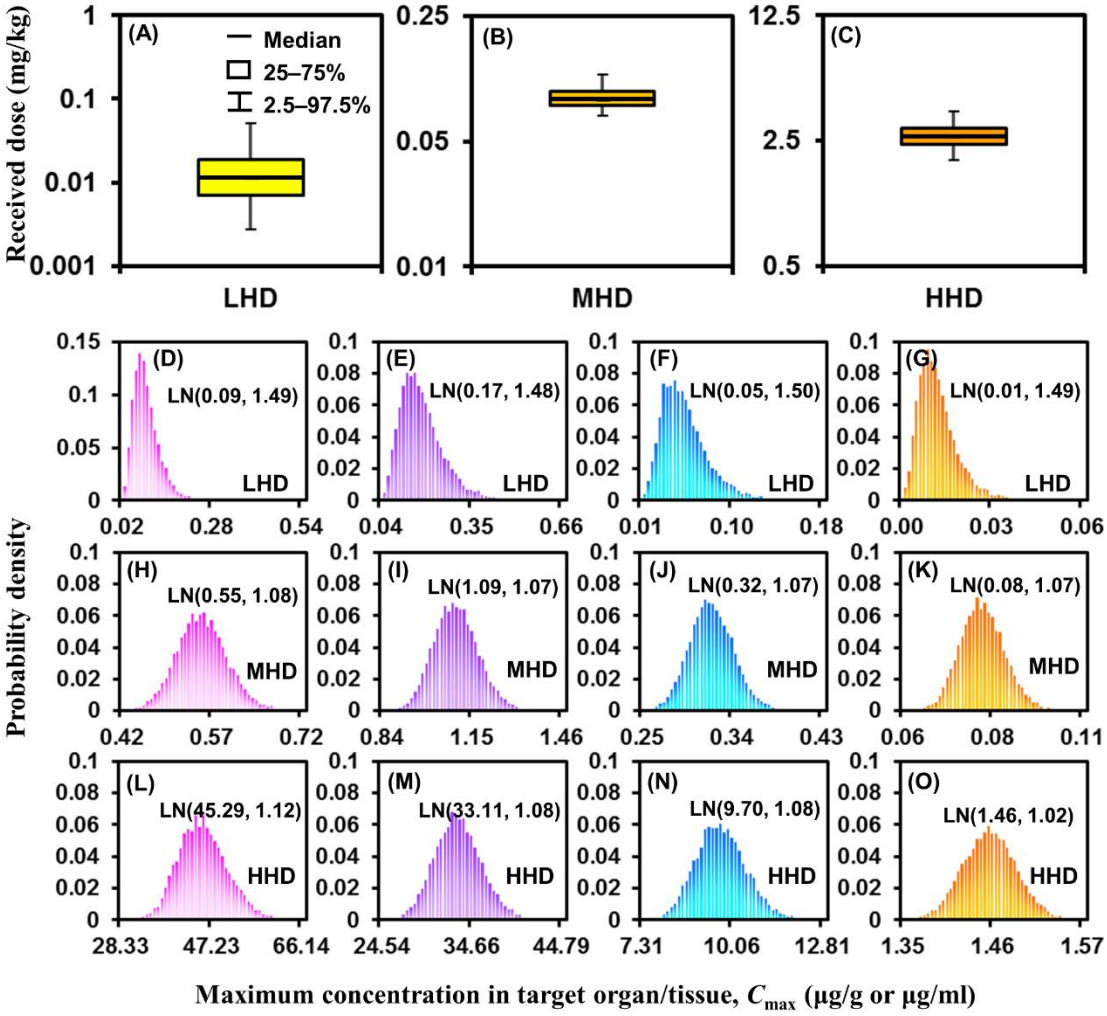

Figure S3. PBPK model-predicted internal organ concentrations of AuNPs. A, B, and C represent low, medium, and high scaled human doses (LHD, MHD, and HHD), respectively. D-O represent maximum internal concentrations in liver (pink) (D, H, L), venous plasma (purple) (E, I, M), kidney (blue) (F, J, N), and skin (orange) (G, K, O) estimated from human AuNP-PBPK model within 24 h after intravenous injection with LHD, MHD, and HHD, respectively.

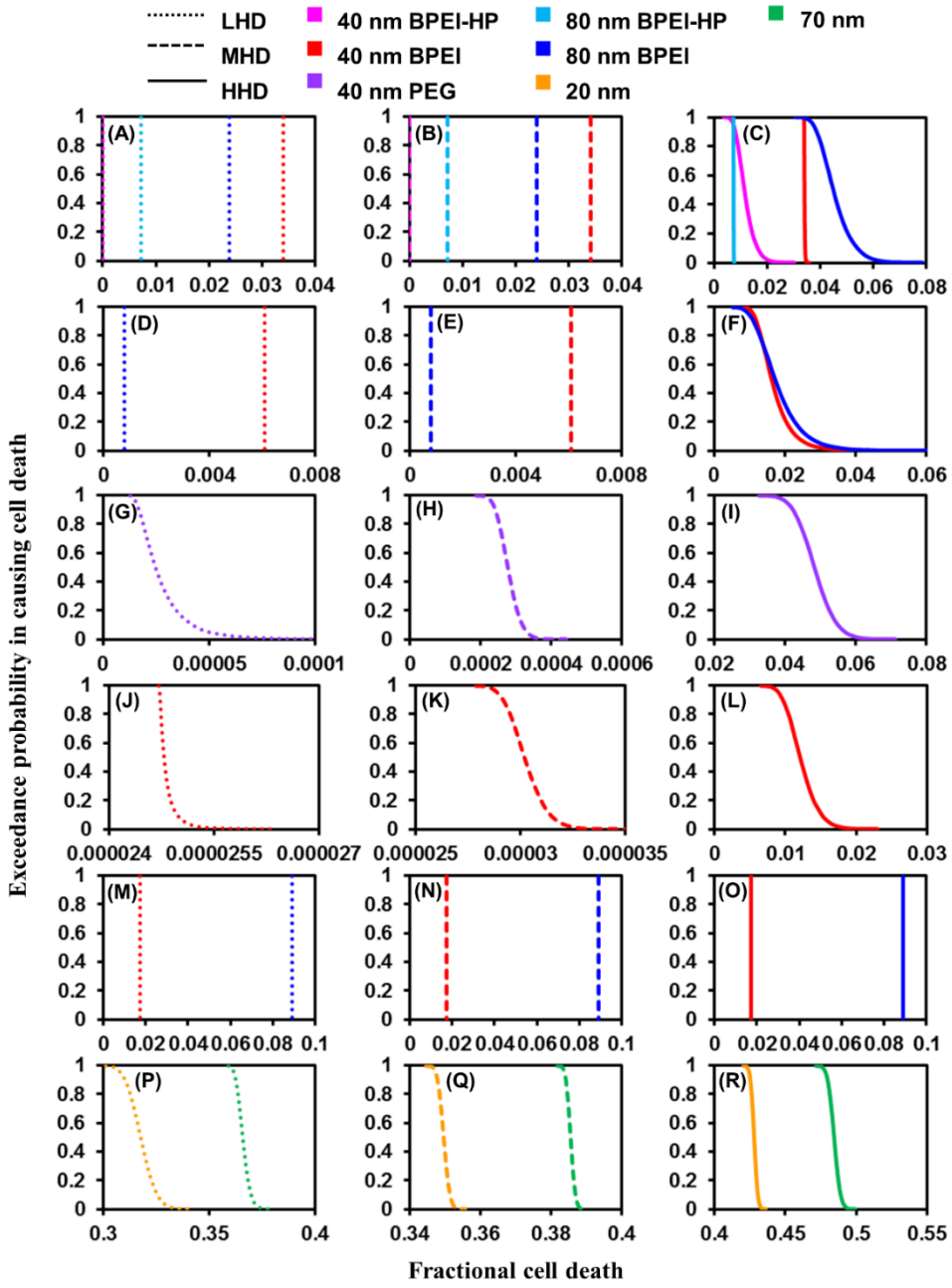

Figure S4. Exceedance risk profiles of internal concentration-associated cell death fraction in hepatocytes (A–C), HUVEC (D–I), HRPTEC (J–L), keratinocytes (M–O), and PMNs (P–R) given low (dotted line), medium (dashed line), high (solid line) scaled intravenous doses.

Table S1. Summary of selected *in vitro* studies used for dose-response analyses.

Human cell type	Size and surface coating of AuNPs	Cell density and incubated medium	Exposed AuNP concentration (μg/ml)	Incubated duration	Detection reagent/ method/instrument	Reference
Keratinocytes	40, 80 nm; BPEI, LA, PEG	10^4/96-well KGM-Gold™	12.5–100	24, 48 h	AlamarBlue/fluorescence microplate reader	Li and Monteiro-Riviere (2016)
Hepatocytes	40, 80 nm; BPEI, LA, PEG coated w/ HP or HSA	6×10^4/96-well Williams' medium E	0–400	24 h	AlamarBlue/fluorescence microplate reader	Choi et al. (2017)
HUVEC	40, 80 nm; BPEI, LA, PEG coated w/ HP or HSA	10^4/96-well EGM-2	0–100	24 h	AlamarBlue/fluorescence microplate reader	Chandran et al. (2017)
HRPTEC	40, 80 nm; BPEI, LA, PEG coated w/ HP or HSA	1.25×10^4/96-well EpiCM	0–200	24 h	AlamarBlue/fluorescence microplate reader	Ortega et al. (2017)
PMNs	20, 70 nm; NA	10^7/96-well RPMI-1640	0–100	24 h	Hema 3/cytology light microscopy	Noël et al. (2016)

Abbreviations: BPEI, branched polyethylenimine; LA, lipoic acid; PEG, polyethylene glycol; HP, human plasma proteins; HSA, human serum albumin; HRPTEC, human renal proximal tubule epithelial cells; HUVEC, human umbilical vein endothelial cells; PMN, polymorphonuclear neutrophil cells; NA, not available.

Table S2. Parameters used in *in vitro* sedimentation, diffusion and dosimetry (ISDD) model and estimated deposited fractions of AuNPs.

Size/surface coating of AuNPs	Hydrodynamic diameter in the DI water (nm) [a]	Hydrodynamic diameter in the medium at 37ºC (nm) [a]	Density of AuNPs (g/mL)	Fractal dimension (DF) [b]	Packing factor (PF) [b]	Viscosity of medium at 37ºC (N s/m^2) [b]	Density of medium (g/mL) [a]	Medium height (cm) [a]	Deposited fraction of AuNPs at 6, 12, and 24 h
40 nm; BPEI	59.4 ± 0.2	177.7 ± 3.3							0.41/0.79/1
80 nm; BPEI	118.9 ± 0.8	150.3 ± 1.1							0.91/1/1
40 nm; LA	48.7 ± 0.3	63.9 ± 0.4	19.32	2.3	0.637	0.00069	1	0.3125	0.30/0.52/0.83
80 nm; LA	103.8 ± 4.0	123.2 ± 0.6							0.83/1/1
40 nm; PEG	71.1 ± 0.2	64.1 ± 0.5							0.30/0.52/0.83
80 nm; PEG	133.1 ± 0.8	126.7 ± 0.9							0.84/1/1

[a] Reported as average values of hydrodynamic diameter (mean ± SD) that were adopted from Choi et al. (2017).

[b] Defaulted values adopted from Hinderliter et al. (2010).

Table S3. Summary of intravenously (IV) administered dosages of AuNPs applied in animal studies and associated scaled dosages that were implemented in human PBPK modeling.

Animal	Size/coating/modification of AuNPs	IV dosage (mg/kg)		Dosing level [b]	Detection method	Reference
		Animal	Human [a]			
Adult rats	1.4, 2.8, 5, 18, 80, 200 nm; TPPMS, TGA, CA	0.005–0.3	0.001–0.05	Low	NAA	Hirn et al. (2011)
Adult mice	50, 80, 100, 150 nm; PEG	0.5–0.6	0.04–0.05	Medium	NAA	Bergen et al. (2006)
Adult mice	Nanorod: 65 nm; PEG	1.2–2.7	0.1–0.2	Medium	ICP-MS	Niidome et al. (2006)
Adult mice	2, 40 nm; citrate	0.6–3.2	0.05–0.3	Medium	AMG	Sadauskas et al. (2007)
Adult rats	10, 50, 100, 250 nm; NA	0.3–0.4	0.06–0.08	Medium	ICP-MS	De Jong et al. (2008)
Adult mice	13 nm; PEG	0.2–4.3	0.01–0.3	Medium	ICP-MS	Cho et al. (2009)
Adult rats	18.4 nm; citrate	0.6–1.0	0.1–0.2	Medium	GF-AAS	Morais et al. (2012)
Adult mice/rats	Nanorod: 60 nm; PEG	0.1	0.01–0.02	Medium	AAS	El-Sayed et al. (2013)
Adult mice	110 nm; PEG	10.3 ± 1.3	0.8 ± 0.1	High	NAA	James et al. (2007)
Adult mice	2 – 20 nm; GSH, pMBA	36.9–86.4	2.9–6.9	High	ICP-MS	Wong et al. (2013)

[a] Human dosages were scaled from animal IV dosages based on conversion factors adopted from Nair and Jacob (2016).
[b] Administered dosing levels were classified based on Khlebtsov and Dykman (2011).
Abbreviations: AAS, atomic absorption spectrometry; AMG, autometallography; CA, cysteamine (2-aminoethanethiol); GF-AAS, graphite furnace atomic absorption spectrometry; GSH, glutathione; ICP-MS, inductively coupled plasma mass spectrometry; NA, not available; NAA, neutron activation analysis; PEG, polyethylene glycol; pMBA, *p*-mercaptobenzoic acid; TGA, thioglycoloic acid (mercaptoacetic acid); TPPMS, triphenylphosphine m-monosulfonate.

Table S4. Fitted parameters (mean ± SE) of the selected dose-response models for describing the relationship between exposure concentration and fractional cell death in human hepatocytes.

Size/surface coating of AuNPs	Model	E_{min}	E_{max}	EC_{50} [a]	α	β	γ or n	r^2
40 nm; BPEI	Exponential	0.0001 ± 0.06	1	261.86		0.003 ± 0.001*		0.7781***
	Weibull	0.04 ± 0.03	1	184.51		0.005 ± 0.0002***	5.53 ± 1.76*	0.9396***
	Logistic	0.03 ± 0.03	1	183.97	7.64 ± 2.31**	0.04 ± 0.01**		0.9391***
	Hill	0.03 ± 0.02	1	185.01 ± 7.89***			6.16 ± 1.86**	0.9428***
80 nm; BPEI	Exponential	0.00001 ± 0.05	1	231.67		0.003 ± 0.001***		0.8401***
	Weibull	0.002 ± 0.04	1	213.19		0.004 ± 0.0004***	1.59 ± 0.34***	0.8908***
	Logistic	0.05 ± 0.04	1	191.98	5.88 ± 1.69**	0.03 ± 0.009**		0.8869***
	Hill	0.02 ± 0.04	1	210.07 ± 15.52***			2.46 ± 0.57***	0.8977***
40 nm; BPEI-HP	Exponential	0.0001 ± 0.08	1	261.86		0.003 ± 0.001*		0.6359**
	Weibull	0.0001 ± 0.04	1	255.73		0.003 ± 0.0003***	2.11 ± 0.50**	0.8916***
	Logistic	0.00001 ± 0.09	1	228.73	4.41 ± 2.75**	0.02 ± 0.01		0.7774**
	Hill	0.00001 ± 0.03	1	273.30 ± 23.36***			2.47 ± 0.45***	0.9468***
80 nm; BPEI-HP	Exponential	0.00001 ± 0.03	1	1059.87		0.001 ± 0.0003*		0.5616***
	Weibull	0.007 ± 0.004	1	394.52		0.002 ± 0.00003***	3.70 ± 0.27***	0.9887***
	Logistic	0.001 ± 0.006	1	394.97	5.61 ± 0.42***	0.01 ± 0.001***		0.9882***
	Hill	0.007 ± 0.004	1	394.66 ± 5.45***			4.22 ± 0.28***	0.9887***

$^{*}p < 0.05$; $^{**}p < 0.01$; $^{***}p < 0.001$.

[a] Parameter values of EC_{50} for exponential, Weibull, and Logistic models were estimated using TableCurve 2D based on constructed dose-response models.

Abbreviations: E_{min} and E_{max}, minimum and maximum fraction of cell death; EC_{50}, exposure concentration leading to half maximum fractional cell death (μg/ml); α, location parameter for the Logistic model; β: slope parameter in dose-response models; γ, exponent parameter for the Weibull model; n, Hill coefficient or exponent; r^2, coefficient of determination.

Table S5. EC_5 and EC_{10} with mean and 95% CI estimates based on the built dose-response relationships.

Human cell types	Size/surface coating of AuNPs	EC_5 (μg/ml)	EC_{10} (μg/ml)
Hepatocytes	40 nm; BPEI-HP	82.8 (40.2–125.3)	112.0 (81.7–152.8)
	80 nm; BPEI-HP	189.2 (173.4–208.1)	230.3 (215.2–246.6)
	40 nm; BPEI	95.4 (46.5–144.3)	121.1 (89.7–152.4)
	80 nm; BPEI	49.0 (9.5–88.5)	77.3 (30.9–108.8)
HUVEC	40 nm; BPEI	43.7 (37.3–50.2)	51.0 (45.5–55.8)
	80 nm; BPEI	42.3 (33.4–51.2)	49.9 (40.4–56.7)
	40 nm; PEG	33.8 (12.0–55.6)	62.2 (31.4–101.2)
HRPTEC	40 nm; BPEI	18.5 (11.0–26.1)	25.8 (14.2–32.0)
Keratinocytes	40 nm; BPEI	29.7 (23.2–36.2)	38.2 (33.3–43.4)
	80 nm; BPEI	NA	12.8 (0–28.8)

Abbreviations: EC_5 and EC_{10}, exposed concentrations leading to 5% and 10% maximum fractional cell death, respectively; BPEI, branched polyethylenimine; PEG, polyethylene glycol; HP, human plasma proteins; HUVEC, human umbilical vein endothelial cells; HRPTEC, human renal proximal tubule epithelial cells; NA, not available.

Human PBPK model code for AuNPs

{{AuNP-PBPK model for humans extrapolated from rats with the main model code adopted from Lin et al. (2016a) and incorporated with Monte Carlo simulation for Lognormally distributed intravenous (IV) dosages to estimate distribution profiles of internal AuNP exposure concentration}}

```
METHOD RK4

STARTTIME = 0
STOPTIME = 24
DT = 0.00125
DTOUT = 0.005

; Blood flow rate (Fraction of cardiac output, unitless)
QCC = 16.5              ; Cardiac output (L/h/kg^0.75) (Brown et al.,1997)
QLC = 0.227             ; Fraction of blood flow to liver (Brown et al.,1997)
QBRC = 0.114            ; Fraction of blood flow to brain (Brown et al., 1997)
QKC = 0.175             ; Fraction of blood flow to kidneys (Brown et al.,1997)
QSC = 0.01375           ; Fraction of blood flow to spleen (Davies and Morris, 1993)

; Tissue volumes (Fraction of body weight, unitless)
BW = 70                 ; Body weight (kg) (Brown et al., 1997)
VLC = 0.0257            ; Liver (Brown et al.,1997)
VBRC = 0.02             ; Brain (Brown et al., 1997)
VKC = 0.0044            ; Kidneys (Brown et al.,1997)
VSC = 0.00257           ; Spleen (Davies and Morris,1993)
VLuC = 0.008            ; Lungs (Brown et al., 1997)
VPlasmaC = 0.079        ; Plasma (Davies and Morris, 1993; Brown et al., 1997)

; Blood volume fraction in organs and tissues (percentage of organs/tissues, unitless)
BVL = 0.11              ; Liver (Brown et al. 1997)
BVBR = 0.04             ; Brain (Brown et al., 1997)
BVK = 0.36              ; Kidneys (Brown et al., 1997)
BVS = 0.3               ; Spleen (Brown et al., 1997, average of mouse, rat, and dog)
BVLu = 0.3867           ; Lungs (Brown et al., 1997, average of mouse, rat, and dog)
BVrest = 0.01           ; Rest of body (Brown et al., 1997, assume equal to the muscle)

; Tissue:plasma distribution coefficients (P, unitless); these values were from our published mouse PBPK model for gold nanoparticles (Lin et al., 2016b)
PL = 0.08               ; Liver
PBR = 0.15              ; Brain
PK = 0.15               ; Kidneys
PS = 0.15               ; Spleen
PLu = 0.15              ; Lungs
Prest = 0.15            ; Rest of body

; Membrane-limited permeability coefficient constants (PA, unitless); these values were from our published mouse PBPK model for gold nanoparticles (Lin et al., 2016b)
PALC = 0.001            ; Liver
PABRC = 0.000001        ; Brain
PAKC = 0.001            ; Kidneys
PASC =0.001             ; Spleen
PALuC = 0.001           ; Lungs
PArestC = 0.000001      ; Rest of body
```

; Endocytic parameters; RES represent phagocytic cells; L, S, K, Lu, rest represent liver, spleen, kidneys, lungs, and rest of body, respectively.

```
KLRESrelease = 0.025      ; Release rate constant of phagocytic cells (h^-1)
KLRESmax = 20             ; Maximum uptake rate constant of phagocytic cells (h^-1)
KLRES50 = 24              ; Time reaching half maximum uptake rate (h)
KLRESn = 0.5              ; Hill coefficient (unitless)
ALREScap = 195            ; Uptake capacity per tissue weight (µg/g tissue)

KSRESrelease = 0.09       ; Release rate constant of phagocytic cells (h^-1)
KSRESmax = 10             ; Maximum uptake rate constant of phagocytic cells (h^-1)
KSRES50 = 24              ; Time reaching half maximum uptake rate (h)
KSRESn = 0.5              ; Hill coefficient (unitless)
ASREScap = 150            ; Uptake capacity per tissue weight (µg/g tissue)

KKRESrelease = 0.0075     ; Release rate constant of phagocytic cells (h^-1)
KKRESmax = 0.5            ; Maximum uptake rate constant of phagocytic cells (h^-1)
KKRES50 = 24              ; Time reaching half maximum uptake rate (h)
KKRESn = 0.5              ; Hill coefficient (unitless)
AKREScap = 330            ; Uptake capacity per tissue weight (µg/g tissue)

KLuRESrelease = 0.07      ; Release rate constant of phagocytic cells (h^-1)
KLuRESmax = 1             ; Maximum uptake rate constant of phagocytic cells (h^-1)
KLuRES50 = 24             ; Time reaching half maximum uptake rate (h)
KLuRESn = 0.5             ; Hill coefficient (unitless)
ALuREScap = 150           ; Uptake capacity per tissue weight (µg/g tissue)

KrestRESrelease = 0.1     ; Release rate constant of phagocytic cells (h^-1)
KrestRESmax = 80          ; Maximum uptake rate constant of phagocytic cells (h^-1)
KrestRES50 = 24           ; Time reaching half maximum uptake rate (h)
KrestRESn = 0.5           ; Hill coefficient (unitless)
ArestREScap = 1.5         ; Uptake capacity per tissue weight (µg/g tissue)

; Biliary excretion
KbileC = 0.0008           ; Biliary clearance (L/hr/kg^0.75)
                          ; L/hr/kg changed to L/h/kg^0.75 for interspecies extrapolation

; Urine excretion
KurineC = 0.0008          ; Urine clearance (L/hr/kg^0.75)
                          ; L/hr changed to L/h/kg^0.75 for interspecies extrapolation

; IV dosing
Timeiv = 0.005            ; IV infusion time (h), set, approximately 15-20 seconds, on average 18 sec
PDOSEiv = 0.001286        ; mg/kg

; Low IV dose (<0.1 mg/kg in animal dose)
LDM = 0.0817                                          ; low animal dose (mean) (mg/kg)
LDSD = 0.0699                                         ; low animal dose (SD) (mg/kg)
LDLOGM = LOGN(LDM^2/(LDM^2+LDSD^2)^0.5)               ; logarithmized animal dose (mean) (mg/kg)
LDLOGSD = (LOGN(1+LDSD^2/LDM^2))^0.5                  ; logarithmized animal dose (SD) (mg/kg)
LPDOSEiv = EXP(NORMAL(LDLOGM, LDLOGSD))               ; lognormally distributed animal dose

; Medium IV dose (0.1-10 mg/kg in animal dose)
MDM = 0.87                                            ; medium animal dose (mean) (mg/kg)
MDSD = 0.16                                           ; medium animal dose (SD) (mg/kg)
MDLOGM = LOGN(MDM^2/(MDM^2+MDSD^2)^0.5)               ; logarithmized animal dose (mean) (mg/kg)
```

```
MDLOGSD = (LOGN(1+MDSD^2/MDM^2))^0.5            ; logarithmized animal dose (SD) (mg/kg)
MPDOSEiv = EXP(NORMAL(MDLOGM, MDLOGSD))         ; lognormally distributed animal dose

; High IV dose (>10 mg/kg in animal dose)
HDM = 33.81                                     ; high animal dose (mean) (mg/kg)
HDSD = 5.33                                     ; high animal dose (SD) (mg/kg)
HDLOGM = LOGN(HDM^2/(HDM^2+HDSD^2)^0.5)         ; logarithmized animal dose (mean) (mg/kg)
HDLOGSD = (LOGN(1+HDSD^2/HDM^2))^0.5            ; logarithmized animal dose (SD) (mg/kg)
HPDOSEiv = EXP(NORMAL(HDLOGM, HDLOGSD))         ; lognormally distributed animal dose

; Scaled parameters
; Cardiac output and regional blood blow (L/h)
QC = QCC*BW^0.75                                ; Cardiac output
QL = QC*QLC                                     ; Blood flow to liver
QBR = QC*QBRC                                   ; Blood flow to brain
QK = QC*QKC                                     ; Blood flow to kidneys
QS = QC*QSC                                     ; Blood flow to spleen
Qrest = QC-QL-QBR-QK-QS                         ; Blood flow to rest of body
Qbal = QC-QL-QBR-QK-QS-Qrest                    ; Blood flow balance equation

; Tissue volumes (L)
VL = BW*VLC                                     ; Liver
VBR = BW*VBRC                                   ; Brain
VK = BW*VKC                                     ; Kidneys
VS = BW*VSC                                     ; Spleen
VLu = BW*VLuC                                   ; Lungs
VPlasma = BW*VPlasmaC                           ; Plasma
Vrest = BW-VL-VBR-VK-VS-VLu-VPlasma             ; Rest of body
Vbal = BW-VL-VBR-VK-VS-VLu-VPlasma-Vrest        ; Tissue volume balance equation

; Capillary blood and tissue interstitium volume in each tissue (L)
VLb = VL*BVL                    ; Weight/volume of capillary blood in liver compartment
VLt = VL-VLb                    ; Weight/volume of tissue in liver compartment
VBRb = VBR*BVBR                 ; Weight/volume of capillary blood in brain compartment
VBRt = VBR-VBRb                 ; Weight/volume of tissue in brain compartment
VKb = VK*BVK                    ; Weight/volume of capillary blood in kidney compartment
VKt = VK-VKb                    ; Weight/volume of tissue in kidney compartment
VSb = VS*BVS                    ; Weight/volume of capillary blood in spleen compartment
VSt = VS-VSb                    ; Weight/volume of tissue in spleen compartment
VLub = VLu*BVLu                 ; Weight/volume of capillary blood in lung compartment
VLut = VLu-VLub                 ; Weight/volume of tissue in lung compartment
Vrestb = Vrest*BVrest           ; Weight/volume of capillary blood in rest of body compartment
Vrestt = Vrest-Vrestb           ; Weight/volume of tissue in rest of body compartment

; Permeability coefficient-surface area cross-product (L/h)
PAL = PALC*QL                   ; Liver
PABR = PABRC*QBR                ; Brain
PAK = PAKC*QK                   ; Kidneys
PAS = PASC*QS                   ; Spleen
PALu = PALuC*QC                 ; Lungs
PArest = PArestC*Qrest          ; Rest of body

; Endocytosis rate (h^-1)
KLRESUP = (KLRESmax*TIME^KLRESn)/
(KLRES50^KLRESn+TIME^KLRESn)*(1-(ALRES/(ALREScap*VL)))          ; Liver
```

```
KSRESUP = (KSRESmax*TIME^KSRESn)/
(KSRES50^KSRESn+TIME^KSRESn)*(1-(ASRES/(ASREScap*VS)))                    ; Spleen
KKRESUP = (KKRESmax*TIME^KKRESn)/
(KKRES50^KKRESn+TIME^KKRESn)*(1-(AKRES/(AKREScap*VK)))                    ; Kidneys
KLuRESUP = (KLuRESmax*TIME^KLuRESn)/
(KLuRES50^KLuRESn+TIME^KLuRESn)*(1-(ALuRES/(ALuREScap*VLu)))              ; Lungs
KrestRESUP = (KrestRESmax*TIME^KrestRESn)/
(KrestRES50^KrestRESn+TIME^KrestRESn)*(1-(ArestRES/(ArestREScap*Vrest)))  ; Rest of body

; IV Dosing scenarios
DOSEiv = PDOSEiv*BW                  ; dose amount (mg)
IVR = DOSEiv/Timeiv                  ; dosing rate (mg/h)
RIV = IVR*(1.-step(1,Timeiv))        ; scenario of dosing rate (mg/h)
d/dt(AIV) = RIV
init AIV = 0

LDOSEiv = LPDOSEiv*BW                ; low amount of dose (mg)
LIVR = LDOSEiv/Timeiv                ; low dosing rate (mg/h)
LRIV = LIVR*(1.-step(1,Timeiv))      ; scenario of low dosing rate (mg/h)
d/dt(AIVL) = LRIV
init AIVL = 0

MDOSEiv = MPDOSEiv*BW                ; medium amount of dose (mg)
MIVR = MDOSEiv/Timeiv                ; medium dosing rate (mg/h)
MRIV = MIVR*(1.-step(1,Timeiv))      ; scenario of medium dosing rate (mg/h)
d/dt(AIVM) = MRIV
init AIVM = 0

HDOSEiv = HPDOSEiv*BW                ; high amount of dose (mg)
HIVR = HDOSEiv/Timeiv                ; high dosing rate (mg/h)
HRIV = HIVR*(1.-step(1,Timeiv))      ; scenario of high dosing rate (mg/h)
d/dt(AIVH) = HRIV
init AIVH = 0

; Elimination
Kbile = KbileC*BW^0.75               ; allometric biliary excretion rate (L/h)
Kurine = KurineC*BW^0.75             ; allometric urinary excretion rate (L/h)

{Blood compartment}
; CA = Arterial blood concentration (mg/L or µg/mL)
RA = QC*CVLu - QC*CA
d/dt(AA) = RA
init AA = 0
CA = AA/(VPlasma*0.2)

; CV = Venous blood concentration (mg/L or µg/mL)
RV = QL*CVL + QBR*CVBR + QK*CVK + Qrest*CVrest + LRIV - QC*CV
d/dt(AV) = RV
init AV = 0
CV = AV/(VPlasma*0.8)

APlasma = AA+AV
CPlasma = APlasma/VPlasma
```

```
{Lung compartment}
; Membrane-limited model
RLub = QC*(CV-CVLu) - PALu*CVLu + (PALu*CLut)/PLu + RLuRESrelease -KLuRESup*ALub
d/dt(ALub) = RLub
init ALub = 0
CVLu = ALub/VLub

RLut = PALu*CVLu - (PALu*CLut)/PLu
d/dt(ALut) = RLut
init ALut = 0
CLut = ALut/VLut
ALutotal = ALub+ALut
CLu = ALutotal/VLu

RLuRES = KLuRESUP*ALub-KLuRESrelease*ALuRES
RLuRESUP = KLuRESUP*ALub
RLuRESrelease = KLuRESrelease*ALuRES
d/dt(ALuRES) = RLuRES
init ALuRES = 0

CLung = (ALutotal+ALuRES)/VLu
CLungtissue = (ALut+ALuRES)/VLut
ALungtissue = ALut+ALuRES

{Brain compartment}
; Membrane-limited model
RBRb = QBR*(CA-CVBR) - PABR*CVBR + (PABR*CBRt)/PBR
d/dt(ABRb) = RBRb
init ABRb = 0
CVBR = ABRb/VBRb

RBRt = PABR*CVBR - (PABR*CBRt)/PBR
d/dt(ABRt) = RBRt
init ABRt = 0

CBRt = ABRt/VBRt
ABRtotal = ABRb+ABRt
CBR = ABRtotal/VBR

{Rest of body compartment}
; Membrane-limited model
Rrestb = Qrest*(CA-CVrest)-PArest*CVrest+(PArest*Crestt)/Prest+RrestRESrelease-KrestRESUP*Arestb
d/dt(Arestb) = Rrestb
init Arestb = 0
CVrest = Arestb/Vrestb

Rrestt = PArest*CVrest - (PArest*Crestt)/Prest
d/dt(Arestt) = Rrestt
init Arestt = 0
Crestt = Arestt/Vrestt
Aresttotal = Arestb+Arestt
Crest = Aresttotal/Vrest

RrestRES = KrestRESUP*Arestb-KrestRESrelease*ArestRES
RrestRESUP = KrestRESUP*Arestb
```

```
RrestRESrelease = KrestRESrelease*ArestRES
d/dt(ArestRES) = RrestRES
init ArestRES = 0

Crestall = (Aresttotal+ArestRES)/Vrest
Cresttissue = (Arestt+ArestRES)/Vrestt
Aresttissue = Arestt+ArestRES

{Kidney compartment}
; Membrane-limited model
RKb = QK*(CA-CVK) - PAK*CVK + (PAK*CKt)/PK - Rurine + RKRESrelease - KKRESUP*AKb
d/dt(AKb) = RKb
init AKb = 0
CVK = AKb/VKb

RKt = PAK*CVK - (PAK*CKt)/PK
d/dt(AKt) = RKt
init AKt = 0
CKt = AKt/VKt
AKtotal = AKb+AKt
CK = AKtotal/VK

RKRES = KKRESUP*AKb-KKRESrelease*AKRES
RKRESUP = KKRESUP*AKb
RKRESrelease = KKRESrelease*AKRES
d/dt(AKRES) = RKRES
init AKRES = 0

CKidney = (AKtotal+AKRES)/VK
CKidneytissue = (AKt+AKRES)/VKt
AKidneytissue = AKt+AKRES

; Urinary excretion
Rurine = Kurine*CVK ;mg/h
d/dt(Aurine) = Rurine
init Aurine = 0

{Spleen compartment}
; Membrane-limited model
RSb = QS*(CA-CVS) - PAS*CVS + (PAS*CSt)/PS + RSRESrelease - KSRESUP*ASb
d/dt(ASb) = RSb
init ASb = 0
CVS = ASb/VSb

RSt = PAS*CVS - (PAS*CSt)/PS
d/dt(ASt) = RSt
init ASt = 0
CSt = ASt/VSt
AStotal = ASb+ASt
CS = AStotal/VS

RSRES = KSRESUP*ASb-KSRESrelease*ASRES
RSRESUP = KSRESUP*ASb
RSRESrelease = KSRESrelease*ASRES
```

```
d/dt(ASRES) = RSRES
init ASRES = 0

CSpleen = (AStotal+ASRES)/VS
Cspleentissue = (ASt+ASRES)/VSt
ASpleentissue = ASt+ASRES

{Liver compartment}
; Membrane-limited model
RLb = QL*(CA-CVL) + QS*CVS - PAL*CVL + (PAL*CLt)/PL - Rbile + RLRESrelease - KLRESUP*ALb
d/dt(ALb) = RLb
init ALb = 0
CVL = ALb/VLb

RLt = PAL*CVL - (PAL*CLt)/PL
d/dt(ALt) = RLt
init ALt = 0
CLt = ALt/VLt
ALtotal = ALb+ALt
CL = ALtotal/VL

RLRES = KLRESUP*ALb-KLRESrelease*ALRES
RLRESUP = KLRESUP*ALb
RLRESrelease = KLRESrelease*ALRES
d/dt(ALRES) = RLRES
init ALRES = 0

CLiver = (ALtotal+ALRES)/VL
CLivertissue = (ALt+ALRES)/VLt
ALivertissue = ALt+ALRES

; Biliary excretion
Rbile = Kbile*CVL ; mg/h
d/dt(Abile) = Rbile
init Abile = 0

{Mass balance}
Tmass = AA+AV+ALtotal+ABRtotal+AKtotal+ALutotal+Aresttotal+AStotal+Abile+Aurine
+ALRES+ASRES+ALuRES+AKRES+ArestRES
Bal = AIVL-Tmass
```

Reference

Bergen JM, von Recum HA, Goodman TT, Massey AP, Pun SH. 2006. Gold nanoparticles as a versatile platform for optimizing physicochemical parameters for targeted drug delivery. Macromol Biosci 6:506–16.

Brown RP, Delp MD, Lindstedt SL, Rhomberg LR, Beliles RP. 1997. Physiological parameter values for physiologically based pharmacokinetic models. Toxicol Ind Health 13:407–84.

Chandran P, Riviere JE, Monteiro-Riviere NA. 2017. Surface chemistry of gold nanoparticles determines the biocorona composition impacting cellular uptake, toxicity and gene expression profiles in human endothelial cells. Nanotoxicology 11:507–19.

Cho WS, Cho M, Jeong J, Choi M, Cho HY, Han BS, et al. 2009. Acute toxicity and pharmacokinetics of 13 nm-sized PEG-coated gold nanoparticles. Toxicol Appl Pharmaco 236:16–24.

Choi K, Riviere JE, Monteiro-Riviere NA. 2017. Protein corona modulation of hepatocyte uptake and molecular mechanisms of gold nanoparticle toxicity. Nanotoxicology 11:64–75.

Davies B, Morris T. 1993. Physiological parameters in laboratory animals and humans. Pharm Res 10:1093–95.

De Jong WH, Hagens WI, Krystek P, Burger MC, Sips AJ, Geertsma RE. 2008. Particle size-dependent organ distribution of gold nanoparticles after intravenous administration. Biomaterials 29:1912–9.

El-Sayed MA, Shabaka AA, El-Shabrawy OA, Yassin NA, Mahmoud SS, El-Shenawy SM,

et al. 2013. Tissue distribution and efficacy of gold nanorods coupled with laser induced photoplasmonic therapy in ehrlich carcinoma solid tumor model. PLoS ONE 8:e76207.

Hinderliter PM, Minard KR, Orr G, Chrisler WB, Thrall BD, Pounds JG, et al. 2010. ISDD: A computational model of particle sedimentation, diffusion and target cell dosimetry for in vitro toxicity studies. Part Fibre Toxicol 7:36.

Hirn S, Semmler-Behnke M, Schleh C, Wenk A, Lipka J, Schäffler M, et al. 2011. Particle size-dependent and surface charge-dependent biodistribution of gold nanoparticles after intravenous administration. Eur J Pharm Biopharm 77:407–16.

James WD, Hirsch LR, West JL, O'Neal PD, Payne JD. 2007. Application of INAA to the build-up and clearance of gold nanoshells in clinical studies in mice. J Radioanal Nucl Chem 271:455–9.

Khlebtsov N, Dykman L. 2011. Biodistribution and toxicity of engineered gold nanoparticles: a review of in vitro and in vivo studies. Chem Soc Rev 40:1647–71.

Li Y, Monteiro-Riviere NA. 2016. Mechanisms of cell uptake, inflammatory potential and protein corona effects with gold nanoparticles. Nanomedicine (Lond) 11:3185–203.

Lin Z, Monteiro-Riviere NA, Kannan R, Riviere JE. 2016a. A computational framework for interspecies pharmacokinetics, exposure and toxicity assessment of gold nanoparticles. Nanomedicine (Lond) 11:107–19.

Lin Z, Monteiro-Riviere NA, Riviere JE. 2016b. A physiologically based pharmacokinetic model for polyethylene glycol-coated gold nanoparticles of different sizes in adult mice. Nanotoxicology 10:162–72.

Morais T, Soares ME, Duarte JA, Soares L, Maia S, Gomes P, et al. 2012. Effect of surface

coating on the biodistribution profile of gold nanoparticles in the rat. Eur J Pharm Biopharm 80:185–93.

Nair AB, Jacob SA. 2016. Simple practice guide for dose conversion between animals and human. J Basic Clin Pharm 7:27–31.

Niidome T, Yamagata M, Okamoto Y, Akiyama Y, Takahashi H, Kawano T, et al. 2006. PEG-modified gold nanorods with a stealth character for in vivo applications. J Control Release 114:343–7.

Noël C, Simard JC, Girard D. 2016. Gold nanoparticles induce apoptosis, endoplasmic reticulum stress events and cleavage of cytoskeletal proteins in human neutrophils. Toxicol In Vitro 31:12–22.

Ortega MT, Riviere JE, Choi K, Monteiro-Riviere NA. 2017. Biocorona formation on gold nanoparticles modulates human proximal tubule kidney cell uptake, cytotoxicity and gene expression. Toxicol In Vitro 42:150–60.

Sadauskas E, Wallin H, Stoltenberg M, Vogel U, Doering P, Larsen A, et al. 2007. Kupffer cells are central in the removal of nanoparticles from the organism. Part Fibre Toxicol 4:10.

Wong OA, Hansen RJ, Ni TW, Heinecke CL, Compel WS, Gustafson DL, et al. 2013. Structure-activity relationships for biodistribution, pharmacokinetics, and excretion of atomically precise nanoclusters in a murine model. Nanoscale 5:10525–33.